# AUXIN RESPONSE FACTOR17 Directly Regulates *MYB108* for Anther Dehiscence[1][OPEN]

**Xiao-Feng Xu,[2] Bo Wang,[2] Yi-Feng Feng,[2] Jing-Shi Xue, Xue-Xue Qian, Si-Qi Liu, Jie Zhou, Ya-Hui Yu, Nai-Yin Yang, Ping Xu, and Zhong-Nan Yang[3,4]**

Shanghai Key Laboratory of Plant Molecular Sciences, College of Life Sciences, Shanghai Normal University, Shanghai 200234, China

**ORCID ID: 0000-0002-5918-2385 (Z.-N.Y.).**

The timely release of mature pollen following anther dehiscence is essential for reproduction in flowering plants. AUXIN RESPONSE FACTOR17 (ARF17) plays a crucial role in pollen wall pattern formation, tapetum development, and auxin signal transduction in anthers. Here, we showed that ARF17 is also involved in anther dehiscence. The Arabidopsis (*Arabidopsis thaliana*) *arf17* mutant exhibits defective endothecium lignification, which leads to defects in anther dehiscence. The expression of *MYB108*, which encodes a transcription factor important for anther dehiscence, was dramatically down-regulated in the flower buds of *arf17*. Chromatin immunoprecipitation assays and electrophoretic mobility shift assays showed ARF17 directly binds to the *MYB108* promoter. In an ARF17-GFP transgenic line, in which ARF17-GFP fully complements the *arf17* phenotype, ARF17-GFP was observed in the endothecia at anther stage 11. The GUS signal driven by the *MYB108* promoter was also detected in endothecia at late anther stages in transgenic plants expressing *promoterMYB108::GUS*. Thus, the expression pattern of both *ARF17* and *MYB108* is consistent with the function of these genes in anther dehiscence. Furthermore, the expression of *MYB108* driven by the *ARF17* promoter successfully restored the defects in anther dehiscence of *arf17*. These results demonstrated that ARF17 regulates the expression of *MYB108* for anther dehiscence. Together with its function in microcytes and tapeta, ARF17 likely coordinates the development of different sporophytic cell layers in anthers. The ARF17-MYB108 pathway involved in regulating anther dehiscence is also discussed.

Anthers produce and release mature pollen for pollination. Anther development starts with the emergence of the stamen primordia in the third whorl of the floral meristem (Goldberg et al., 1993). Arabidopsis (*Arabidopsis thaliana*) anthers consist of an outer epidermis, an endothecium, a middle layer, a tapetum, and an inner microsporocyte (Wilson et al., 2011). The middle layer degenerates at the early stage of anther development (Cecchetti et al., 2017), and the microsporocyte and tapetum are directly involved in pollen formation (Twell, 2011). Microsporocytes undergo meiosis to generate tetrads of haploid microspores, and the tapetum provides necessary materials and nutrients for pollen wall formation and microspore development (Xu et al., 2015). The release of mature pollen depends on anther dehiscence, which requires endothecium lignification and stomium cell degeneration.

Much progress has been made in research related to anther dehiscence in recent years. Defects in anther dehiscence have been observed in mutants of the jasmonic acid (JA) synthesis pathway (Sanders et al., 2000; Stintzi and Browse, 2000; Ishiguro et al., 2001; Park et al., 2002; von Malek et al., 2002). JA biosynthesis is controlled and processed through the *DEFECTIVE ANTHER DEHISCENCE1* (*DAD1*)-*ARABIDOPSIS THALIANA LIPOXYGENASE-ALLENE OXIDE SYNTHASE-ALLENE OXIDE CYCLASE-OXOPHYTODIENOATE REDUCTASE3* (*OPR3*)-*MYB DOMAIN PROTEIN24* (*MYB24*) pathway (Wilson et al., 2011; Huang et al., 2017). For example, *OPR3* encodes a 12-oxophytodienoate reductase, and mutation of *OPR3* leads to defective anther dehiscence, although the timing of endothecium lignification is normal (Cecchetti et al., 2013). *QUARTET2* (*QRT2*), *ARABIDOPSIS DEHISCENCE ZONE POLYGALACTURONASE1* (*ADPG1*), and *ADPG2* encode polygalacturonases, and JA regulates the expression of these genes. The triple mutant of these genes shows defective stomium cell degeneration, which leads to delayed anther dehiscence (Ogawa et al., 2009). Moreover, MYB26 directly regulates the

[1]This work was supported by the National Natural Science Foundation of China (grant nos. 31670314 and 31870296), the Shanghai Sailing Program (grant no. 17YF1414000), and the Shanghai Science and Technology Committee (grant nos. 18DZ2260500 and 17DZ2252700).

[2]These authors contributed equally to the article.

[3]Author for contact: znyang@shnu.edu.cn.

[4]Senior author.

The author responsible for distribution of materials integral to the findings presented in this article in accordance with the policy described in the Instructions for Authors (www.plantphysiol.org) is: Zhong-Nan Yang (znyang@shnu.edu.cn).

Z.-N.Y. led the project; X.-F.X., B.W., Y.-F.F., J.-S.X, X.-X.Q., S.-Q. L., J.Z., Y.-H.Y., and N.-Y.Y. performed the experiments; Z.-N.Y. and X.-F.X. designed the experiments; Z.-N.Y. and X.-F.X. wrote the article; and Z.-N.Y. and P.X. reviewed and edited the article.

[OPEN]Articles can be viewed without a subscription.

www.plantphysiol.org/cgi/doi/10.1104/pp.19.00576

  

expression of *NAC SECONDARY WALL THICKENING PROMOTING FACTOR1* (*NST1*) and *NST2*. Both *myb26* and *nst1 nst2* mutants show defective endothelial lignification and failed anther dehiscence (Steiner-Lange et al., 2003; Mitsuda et al., 2005; Yang et al., 2017).

In addition to JA, another plant hormone, auxin, also plays an important role in anther dehiscence (Cardarelli and Costantino, 2018). In Arabidopsis, the auxin receptors *TRANSPORT INHIBITOR RESPONSE1* (*TIR1*), *AUXIN SIGNALING F BOX PROTEIN1* (*AFB1*), *AFB2*, and *AFB3* are expressed at the late stages of anther development. *tir1 afb1 afb2 afb3* quadruple mutants display earlier anther dehiscence than do wild-type plants (Cecchetti et al., 2008). In rice (*Oryza sativa*), the *ORYZA SATIVA HOMEOBOX1* transcription factor directly suppresses *ORYZA SATIVA YUCCA4* (*OsYUCCA4*) expression and auxin biosynthesis, thus controlling the timing of anther dehiscence. Overexpression of *OsYUCCA4* in *oryza sativa homeobox1* mutants results in anther indehiscence (Song et al., 2018). Auxin response factors (ARFs), together with auxin (Aux)/indole acetic acid repressors, are key components of the auxin signaling pathway (Guilfoyle and Hagen, 2007). In Arabidopsis, there are 23 members of the ARF family (Remington et al., 2004). Anther dehiscence is delayed in *arf1 arf2* mutants (Ellis et al., 2005), and *arf6 arf8* mutants show reduced filament and petal elongation as well as delayed or no dehiscence (Nagpal et al., 2005; Cecchetti et al., 2007; Tabata et al., 2010). In addition, a recent report showed that ARF8.4 directly regulates *MYB26* for endothecium lignification (Ghelli et al., 2018).

ARF17 is important for anther development and pollen formation. In microsporocytes/tetrads, ARF17 directly regulates *CALLOSE SYNTHASE5* (*CALS5*) for pollen wall pattern formation (Yang et al., 2013). In the tapetum, ARF17 expression is under strict control by *MICRORNA160*. ARF17 overexpression leads to defects in tapetum development and male sterility (Wang et al., 2017). In addition to MYB26, MYB108 is involved in anther dehiscence, but its exact function is not clear (Mandaokar and Browse, 2009). In this work, we show ARF17 is also important for anther dehiscence and that it directly regulates the expression of *MYB108* for endothecium lignification during anther dehiscence.

## RESULTS

### Anther Dehiscence Is Defective in *arf17*

ARF17 is a key auxin response factor in anthers as auxin signals are absent in *arf17* mutants (Yang et al., 2013). Here, the results from observations via scanning electron microscopy showed anther dehiscence is defective in *arf17* mutants. Normal anther dehiscence of wild-type plants occurs at anther stage 13 (Sanders et al., 1999) and relies on endothecium lignification, septum degradation, and stomium breakage in the anthers (Wilson et al., 2011). However, the stomium of *arf17* anthers was not completely open (Fig. 1A). Further cytological analysis revealed the details of anther development in the *arf17* mutant, particularly endothecium lignification. Endothecium lignification involves the deposition of pointed bar-like lignocellulosic fibrous bands (Sanders et al., 2000; Scott et al., 2004; Wilson et al., 2011). Observations of serial semithin sections of the anthers showed the absence of fibrous band deposition in the endothecium of *arf17* anthers at stage 12 while the anthers were shriveled (Fig. 1B; Supplemental Fig. S1). In addition, we performed Tinopal staining of semithin sections of *arf17* anthers (Lou et al., 2014). Normal lignified endothecia from wild-type anthers fluoresce after Tinopal staining, but there was no fluorescence in the *arf17* anthers (Fig. 1C). Hence, endothecium lignification required for pollen release was defective in the *arf17* mutant. Using transmission electron microscopy (TEM), we found that the septum is adhesive in *arf17* mutant (Fig. 1D). Hence, all these results indicate endothecium lignification and stomium opening are defective in *arf17* anthers. Stomium opening also requires stomium breakage. *QRT2*, *ADPG1*, and *ADPG2* are involved in stomium breakage during anther dehiscence (Ogawa et al., 2009). The results from reverse transcription quantitative PCR (RT-qPCR) analysis indicated the expression of these genes was not affected in *arf17* anthers (Supplemental Fig. S2), suggesting that the stomium breakage is normal in *arf17* mutants. These results demonstrated that defects in endothecium lignification, instead of stomium cell degeneration, led to anther indehiscence in the *arf17* mutant.

### ARF17 Directly Regulates the Expression of *MYB108*

To understand the mechanisms of ARF17 regulation of endothecium lignification in anther dehiscence, we investigated the putative genes that may be regulated by ARF17. There are 1048 genes that are down-regulated in the *arf17* mutant compared with wild type (Supplemental Table S1). Among those genes, 235 are expressed at the late stage of anther development, according to the Arabidopsis transcriptome database (http://bar.utoronto.ca; Fig. 2A). Furthermore, ARF17 binds the Aux motif (TGTCTC/GAGACA; Yang et al., 2013). Of the 235 genes, 110, including *MYB108*, contained an Aux motif in their promoter (Fig. 2A; Supplemental Table S2). *MYB108* is involved in anther dehiscence (Mandaokar and Browse, 2009). To further understand the expression change of *MYB108* in the *arf17* mutant, we collected wild-type and *arf17* flower buds at different floral stages and performed RT-qPCR analysis. The results

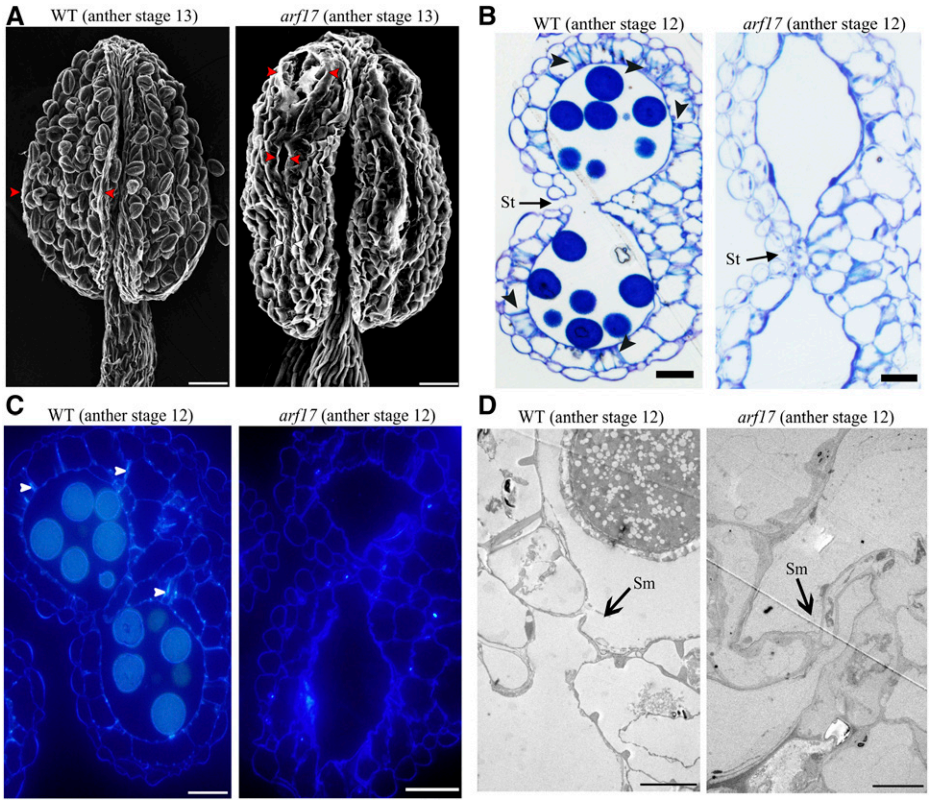


**Figure 1.** Anther indehiscence of *arf17* mutants. A, The opening of anther structures of wild-type (WT) and *arf17* anthers at stage 13 observed via SEM. Bars, 20 $\mu$m. Red arrowheads indicate the stomium opening. B, Semithin sections of anthers of wild-type and *arf17* mutants at stage 12. Bars, 20 $\mu$m. Black arrowheads indicate fibrous bands in the endothecium. C, Ligno-cellulosic fibrous bands in the anthers of wild-type and *arf17* mutants at stage 12, resulting from cytochemical staining of their corresponding semithin sections. White arrowheads indicate fibrous bands in the endothecium. Bars, 20 $\mu$m. D, The phenotype of septum degradation in wild-type and *arf17* anthers at stage 12 observed via TEM. Bars, 5 $\mu$m. The anther developmental stages refer to those of Sanders et al. (1999). St, Stomium; Sm, septum.

verified the dramatic down-regulation of *MYB108* expression in *arf17* buds after stage 10 (Fig. 2B).

There is an intergenic region of approximately 10 kb between *MYB108* (AT3G06490) and its closest locus AT3G06483, which includes the promoter of *MYB108*. The promoter of *MYB108* contains one AuxRE (TGTCTC) located at −3745 to −3751 bp from the start codon. To understand whether ARF17 binds this motif, we performed chromatin immunoprecipitation (ChIP) assays and electrophoretic mobility shift assays (EMSAs). The GFP antibody was used to perform the ChIP analysis using the inflorescence of the ARF17-GFP/*arf17* complementary plant. Our previous work demonstrated ARF17 directly binds the AuxRE motif within the *CALS5* promoter (Yang et al., 2013). Here, the *MYB108-1* primer pair was used to measure the enrichment in ARF17 protein on the AuxRE (TGTCTC) motif within the *MYB108* promoter. We used the *MYB108-2* and *MYB108-3* primer pairs as negative controls to examine the enrichment in the region without the AuxRE motif and AuxRE-like (AGTCTC) motif sequences in the *MYB108* promoter, respectively. ChIP-qPCR experiments indicated ARF17 is enriched in the *MYB108-1* region (Fig. 2C). We then expressed the glutathione *S*-transferase (GST)-ARF17 recombinant protein as previously reported (Yang et al., 2013). A probe containing the AuxRE motif (TGTCTC) in the *MYB108* promoter (MYB108 probe) was used for EMSAs, which showed the ARF17 protein specifically bound to the probe in vitro. When the unlabeled probe was added, the excess competitor reduced the abundance of shifted bands. When the AuxRE motif was mutated in this MYB108 probe, the ARF17 protein did not bind to the mutant MYB108 probe, supporting the binding specificity (Fig. 2D). These results reveal that ARF17 directly binds to the *MYB108* promoter to regulate its expression.

### Delayed Lignification in the Endothecium Leads to Defective Anther Dehiscence in *myb108* Mutants

We obtained a transfer DNA insertion mutant of *MYB108* (SALK_024059) that was previously reported (Mandaokar and Browse, 2009). Its *ARF17* expression was not affected (Supplemental Fig. S3B). The *myb108* mutant was severely sterile at early reproductive stages but was fertile at later reproductive stages (Fig. 3, A–C). Its mature pollen was functional but was not released (Fig. 3, D–G), while the septum and stomium degradation was normal (Supplemental Fig. S3C). During anther development in wild-type plants, the lignification of the endothecium layer appears after anther stage 10 (Sanders et al., 1999; Wilson et al., 2011). We used confocal laser scanning microscopy to observe the lignin autofluorescence in the endothecium layer of wild type, *arf17*, and *myb108* (Auxenfans et al., 2017). The lignin autofluorescence was observed in the endothecia of wild-type anthers at anther stages 11 and 12. However, lignin signal was not observed in *arf17* at either anther stage but was observed in *myb108* at anther stage 12 (Fig. 3H). Thus, *ARF17* is essential for

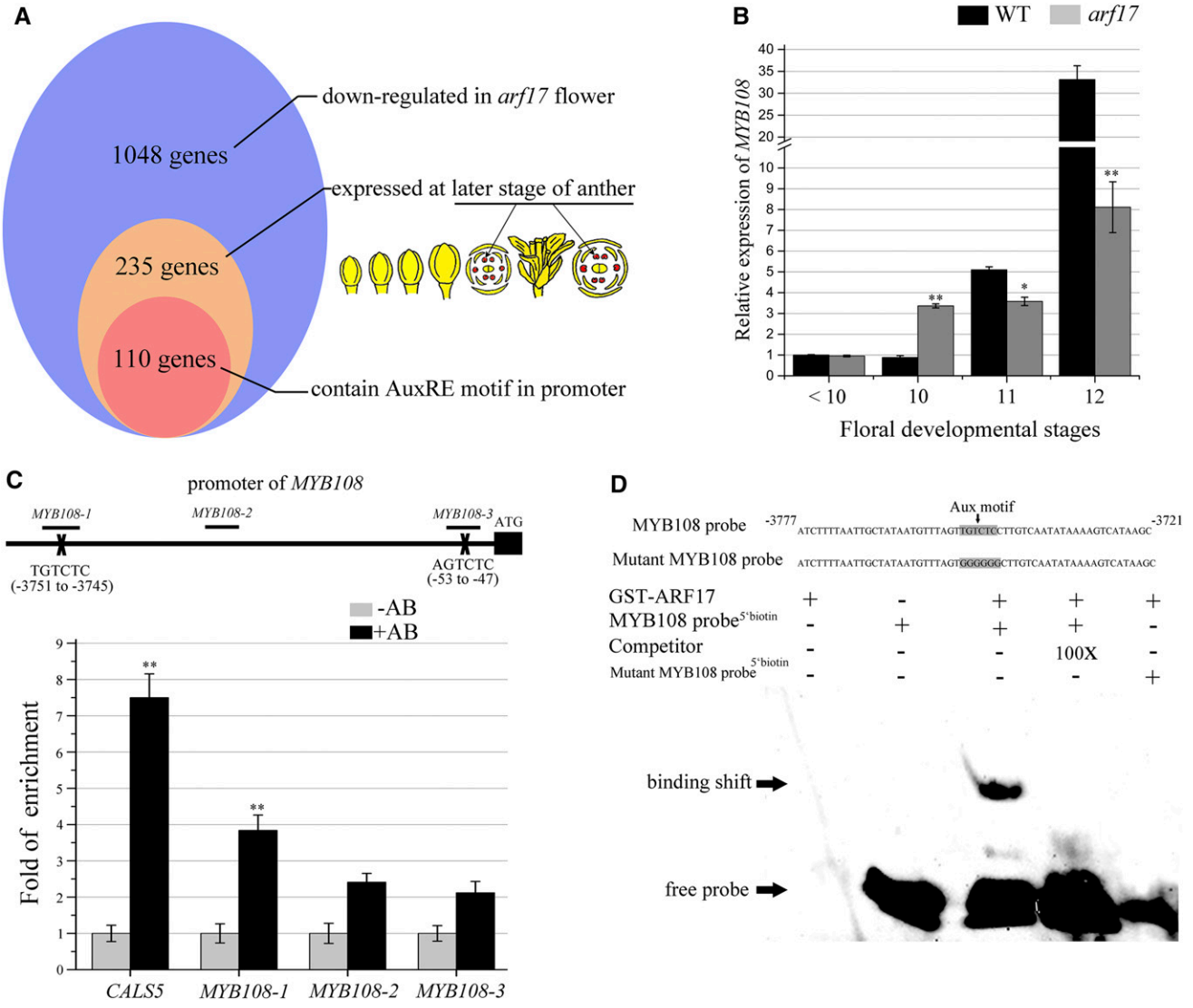


**Figure 2.** ARF17 directly regulates the expression of *MYB108*. A, More than 10% of ARF17-regulated genes contain an AuxRE motif in their promoter. The results of a microarray analysis showed that 1048 genes were down-regulated in the flower buds of the *arf17* mutant compared with wild type (WT; FC > 1.5). Among those genes, 235 were mainly expressed at the late stage of anthers, according to the Arabidopsis electronic fluorescent pictographs browser (Winter et al., 2007). The results from the query of plant cis-acting regulatory DNA elements showed 110 genes contain an AuxRE motif in their promoter (Higo et al., 1999). B, RT-qPCR analysis of *MYB108* expression in wild-type and *arf17* flower buds at different developmental stages. The expression level was normalized to that of *TUB* and compared with the wild type at stages < 10. The floral developmental stages refer to those of Sanders et al. (1999). The error bars indicate SDs and were calculated from three biological replicates. A two-tailed *t* test was used to evaluate statistical significance (*$P < 0.05$; **$P < 0.01$). C, ChIP-qPCR analysis of ARF17 protein enrichment on the promoter region of *MYB108*. The *MYB108-1* promoter region contains the canonical AuxRE sequence (TGTCTC) from −3745 to −3751. The *MYB108-2* and *MYB108-3* regions contain the AuxRE-like sequences TGTCTT from −2125 to −2119 and AGTCTC from −53 to −47, respectively. DNA recovered after the addition of GFP antibody ($AB^+$) and no antibody ($AB^-$) was used as a template. Enrichment of the *MYB108* promoter was confirmed by qPCR using the primer sets *MYB108-1*, *MYB108-2*, and *MYB108-3*, as well as the primer set *CALS5*, which served as the positive control, as described previously (Yang et al., 2013). The relative enrichment is presented compared to that of the $AB^-$ trial of each primer set. The means are shown with ± SDs. A two-tailed *t* test was used to evaluate statistical significance (*$P < 0.05$; **$P < 0.01$). D, The results of EMSAs. GST-ARF17 protein was mixed with a biotin-labeled 60-bp probe containing the AuxRE and 100-fold unlabeled probe as a competitor. The unlabeled competitors reduced the visible shift significantly (arrow). The ARF17 protein could not bind the mutant *MYB108* probe, whose AuxRE motif sequence (TGTCTC) was changed to GGGGGG.

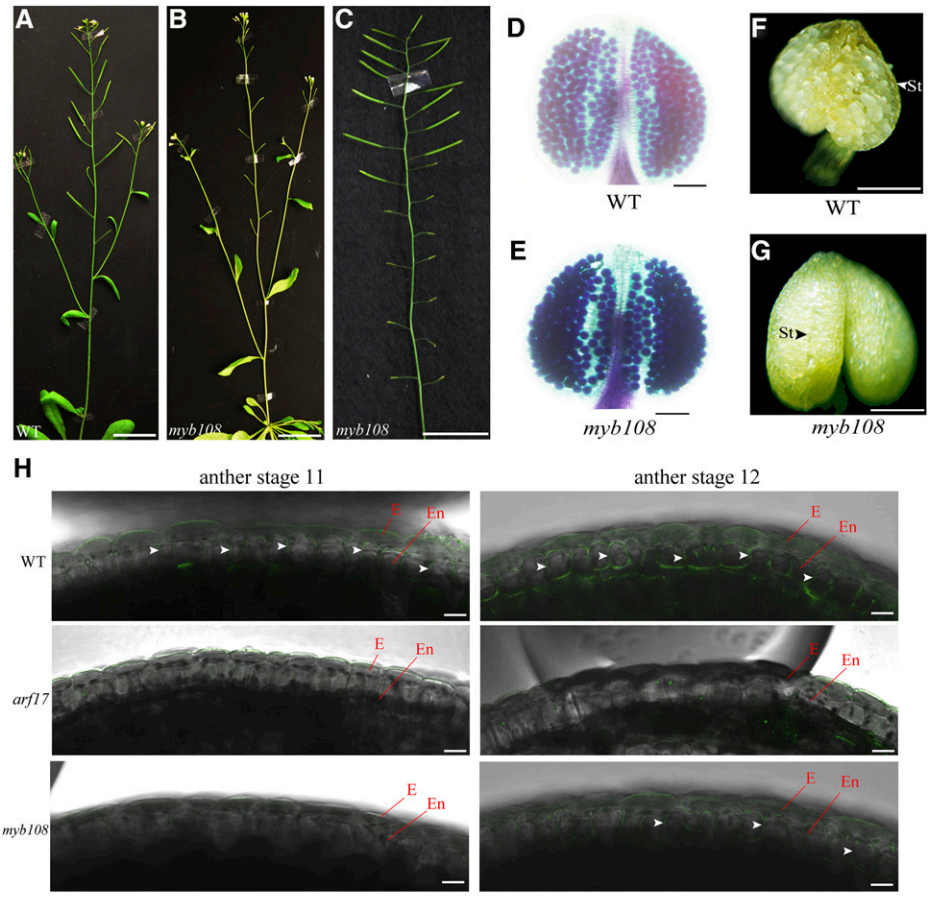


**Figure 3.** Lignification is affected in *myb108* mutants. A to C, Wild type (WT) is fertile (A), whereas *myb108* shows a sterile phenotype at the early reproduction stage (B), but its fertility is restored at the late reproduction stage (C). Bars, 1 cm. D and E, Alexander's staining of wild-type (D) and *myb108* (E) anthers. Bars, 100 mm. F and G, The dehisced anthers of opening flowers in wild type (F). The nondehisced anthers of opening flowers in a *myb108* mutant (G). Bars, 200 $\mu$m. H, The autofluorescence of lignification in the endothecium layer at anther stages 11 and 12 from wild-type, *arf17*, and *myb108* mutants. Anthers were isolated from flower buds of the same size. The images were taken under a fluorescence confocal microscope with the same settings (excitation, 405 nm; emission, 450–550 nm). The white arrowheads indicate lignin autofluorescence signals. Bars, 10 $\mu$m. E, Epidermis; En, endothecium.

endothecium lignification, but normal lignification is delayed in anthers of *myb108*.

### Both ARF17 and MYB108 Are Expressed in the Endothecium

ARF17 is highly expressed in microsporocytes and microgametophytes and weakly expressed in tapeta (Yang et al., 2013; Wang et al., 2017). We used confocal microscopy to observe ARF17-GFP fluorescence in the *promoterARF17::ARF17-GFP/arf17* (*ARF17-GFP/arf17*) complementary line. The endothecium cells contain chloroplasts that showed strong chlorophyll fluorescence. This phenomenon could be used as a cellular marker of endothecium cells. The scanning of anther longitudinal sections at different positions showed ARF17-GFP signals were clearly located in anther endothecia (Fig. 4, A and B). We also generated a *promoterMYB108::GUS* construct and introduced it into wild-type plants. GUS staining showed *MYB108* was expressed in the anthers at later development stages. Paraffin sections of stained anthers revealed the GUS signal was mainly localized to the endothecium layer (Fig. 4C). The expression of ARF17 and MYB108 in the endothecium is in agreement with their function in anther dehiscence.

### The Expression of *MYB108* in *arf17* Rescues Its Anther Dehiscence Phenotype

To understand whether *MYB108* is the major target of ARF17 for anther dehiscence, we expressed *MYB108* in *arf17* mutants. We developed a *promoterARF17::MYB108* construct (Fig. 5A) and introduced it into *arf17* mutants as described previously (Xu et al., 2015). A total of 15 transgenic lines with the *arf17* background (*pARF17::MYB108/arf17*) were identified (Supplemental Fig. S4). These transgenic plants were sterile (Fig. 5, B and C). RT-qPCR analysis showed that the expression level of *MYB108* in the *pARF17::MYB108/arf17* plants was partially restored (Fig. 5D). Observations of semithin sections of the anthers showed the endothecium lignification was restored, although pollen development remained defective. The anthers were no longer shriveled, and stomium opening was also restored (Figs. 1B and 5, E and F). These results demonstrate that *MYB108* plays an important role for ARF17 to regulate endothecium lignification and anther dehiscence.

### The Relationship between *ARF17* and Other Genes Involved in Endothecium Lignification

YUCCA2 (YUC2) and YUC6 are two auxin synthesis enzymes essential for anther development and pollen

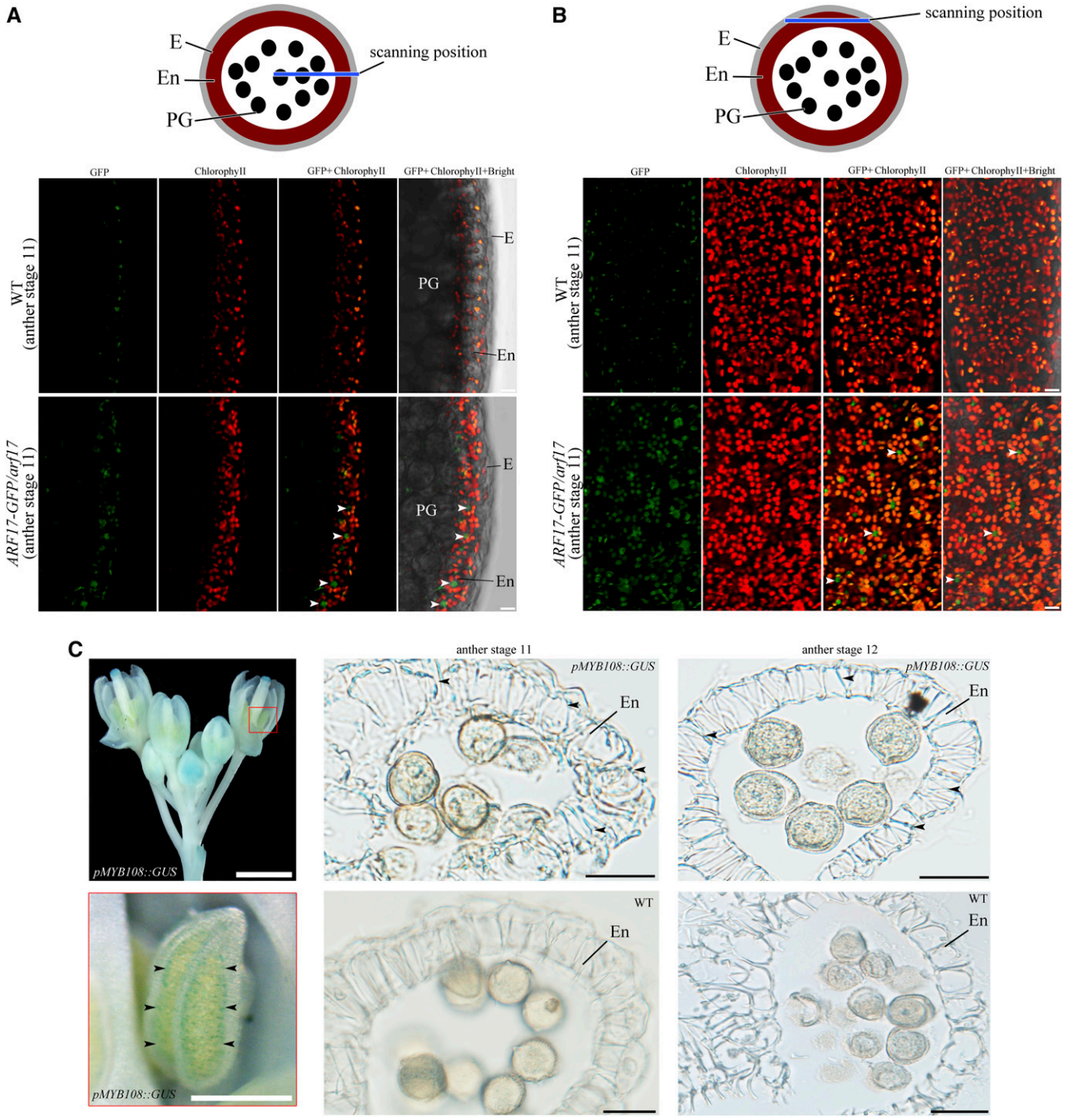


**Figure 4.** The observations of GFP in *ARF17-GFP/arf17* plants and GUS staining in *promoterMYB108::GUS* plants. A and B, The GFP signals in the anther of *promoterARF17::ARF17-GFP/arf17* (*ARF17-GFP/arf17*) and wild-type (WT) plants at anther stage 11. The images were collected when the scanning position was at the cross section of the anthers (A) and endothecium layer (B) under a fluorescence confocal microscope. Bars, 10 $\mu$m. The white arrowhead indicates the ARF17-GFP signals. (C) The expression of the GUS reporter driven by the *MYB108* promoter in the flower and the cross sections of anthers of wild-type and transgenic plants expressing *promoterMYB108::GUS* (*pMYB108::GUS*) at different developmental stages. The GUS activities (blue) were examined using histochemical staining. The black arrowheads indicate the GUS staining in the late stage of anthers. White bars, 1 mm; black bars, 20 $\mu$m. The anther developmental stages refer to those of Sanders et al. (1999). E, Epidermis; En, endothecium; PG, pollen grain.

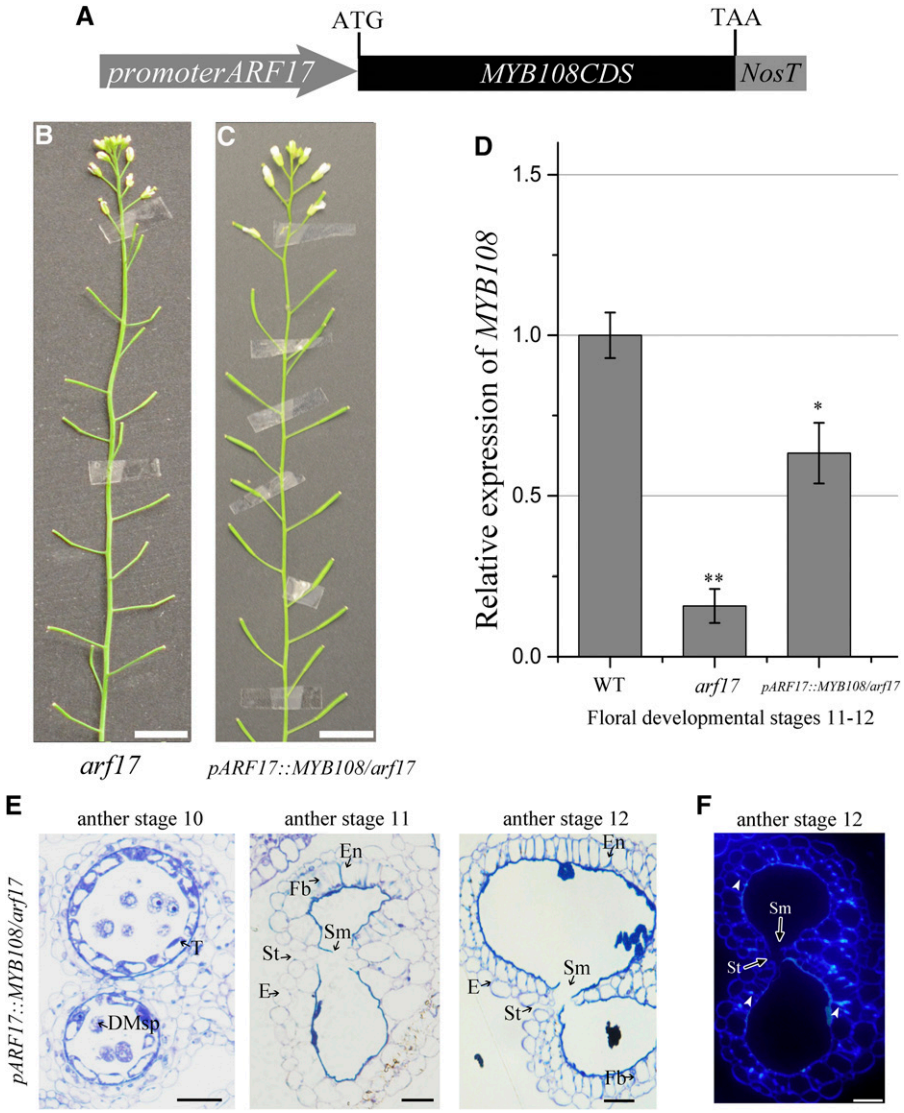


**Figure 5.** *MYB108* expression driven by the *ARF17* promoter in the anthers of *arf17* mutants rescues the anther dehiscence. A, The construct of *promoterARF17::MYB108* (*pARF17::MYB108*). B, The phenotype of an *arf17* mutant. Bars, 2 cm. C, The phenotype of a *promoterARF17::MYB108* transgenic plant in the *arf17* mutant background (*pARF17::MYB108/arf17*). Bars, 2 cm. D, RT-qPCR analysis of *MYB108* expression in wild-type (WT) plants, the *arf17* mutant, and *pARF17::MYB108/arf17* plants. Flower buds at floral developmental stages 11 and 12 were collected for RT-qPCR analysis. The expression level of *MYB108* was normalized to the expression of *TUB*. The error bars indicate SDs among three biological replicates. A two-tailed *t* test was used to evaluate statistical significance ($*P < 0.05$; $**P < 0.01$). E, Semithin sections of the anthers of *pARF17::MYB108/arf17* plants showing anther development at anther stages 10 to 12. The image of the anther semithin section shows the septum degradation and stomium opening that were restored in the *pARF17::MYB108/arf17* plants. Bars, 20 $\mu$m. F, Results from cytochemical staining of the semithin sections of *pARF17::MYB108/arf17* anthers at stage 12. The signal of deposited ligno-cellulosic fibrous bands can be observed at anther stage 12 in *pARF17::MYB108/arf17* plants (white arrowheads). Bars, 20 $\mu$m. The anther and floral developmental stages refer to those of Sanders et al. (1999). DMsp, Degraded microspores; E, epidermis; En, endothecium; Fb, fibrous bands; T, tapetum; St, stomium; Sm, septum.

formation (Cheng et al., 2006; Yao et al., 2018). Although ARF17 is a member of the auxin-responsive factor family, it is unclear if it is responsive to auxin. In the *yuc2 yuc6* mutant, RT-qPCR analysis showed the expression of *ARF17* was up-regulated, while the expression of *MYB108* was significantly down-regulated (Fig. 6A). These suggest that the ARF17-MYB108 pathway is responsive to auxin to regulate endothecium lignification in Arabidopsis. The ARF8-MYB26 pathway was reported to directly regulate *NST1* and *NST2* for endothecium lignification (Yang et al., 2017; Ghelli et al., 2018). The expression of *ARF8* and *MYB26* were slightly up-regulated in *yuc2 yuc6* (Fig. 6A). Their expression was also increased in *arf17*, as well as the expression of *ARF6* (Fig. 6B; Supplemental Fig. S5). However, *NST1* was down-regulated in the *arf17* mutant (Fig. 6C), indicating that it plays a role for ARF17 to regulate endothecium lignification. The JA pathway is involved in anther dehiscence, and OPR3 and DAD1 are two enzymes in the JA pathway. The *opr3* mutant shows defects in stomium opening (Cecchetti et al., 2013), and the expression of *MYB21* and *MYB24* is down-regulated (Huang et al., 2017). In *yuc2 yuc6*, *OPR3* was up-regulated (Fig. 6A), while *DAD1* was not affected (Fig. 6A). *OPR3* was also up-regulated in *arf17* anthers (Fig. 6D). However, *MYB24* was down-regulated at early stages but up-regulated at late stages in the *arf17* mutant (Fig. 6E). The up-regulation of *OPR3* in *arf17* and *yuc2 yuc6* indicates auxin may negatively regulate JA biosynthesis in anther.

## DISCUSSION

Anther dehiscence is one of the key events in plant sexual reproduction (Cardarelli and Costantino, 2018) and involves endothecium lignification and stomium cell degradation (Wilson et al., 2011). Here, we report that ARF17 is a novel regulator of endothecium lignification during anther dehiscence. *MYB108* also plays a

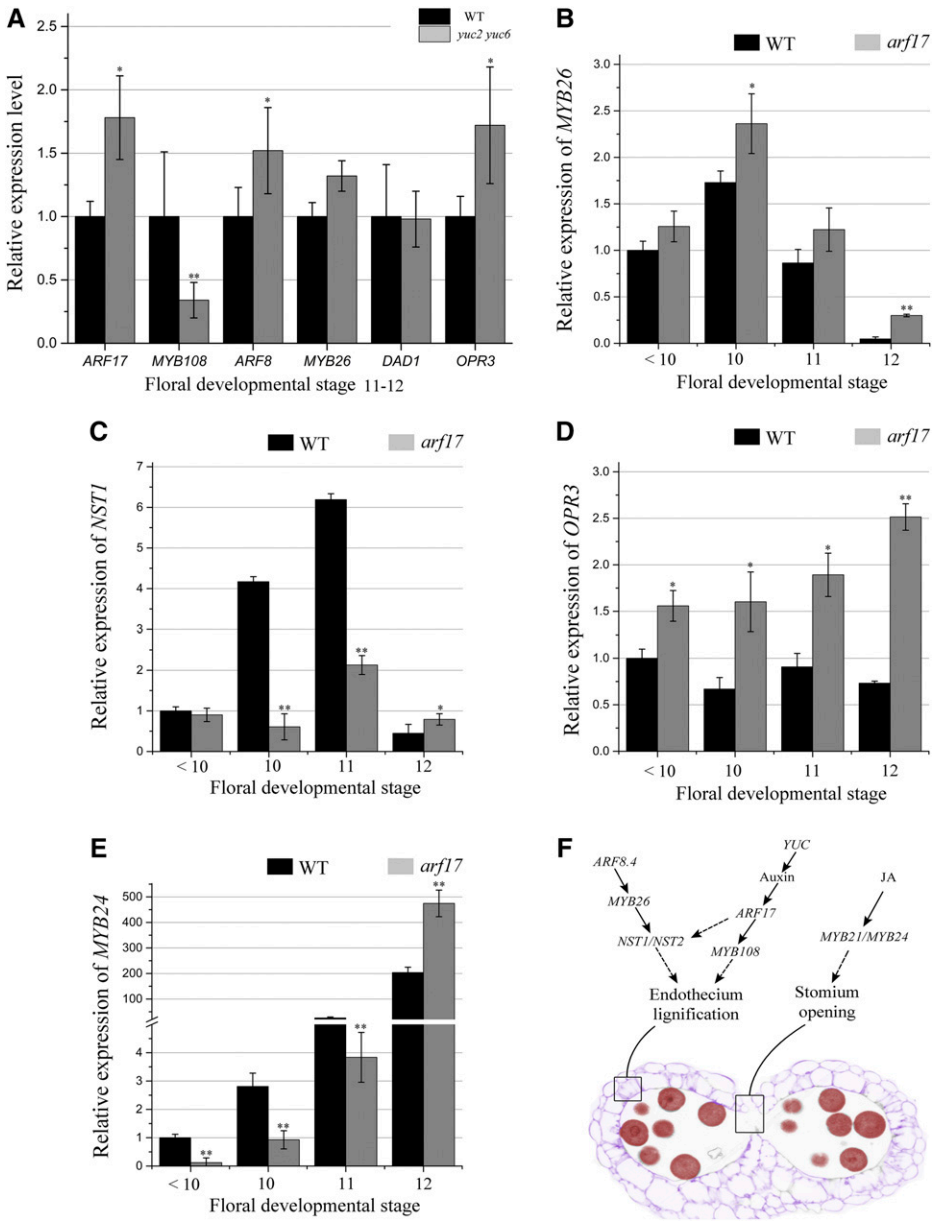


**Figure 6.** The expression of anther dehiscence genes in *arf17* and *yuc2 yuc6* mutants. A, RT-qPCR analysis of the expression of the major genes in the JA and ARF8-MYB26 pathways in wild-type (WT) and *yuc2 yuc6* buds. Flower buds at floral developmental stages 10 to 12 were collected. The expression levels of these genes in wild type were set to 1. B to E, RT-qPCR analysis of the expression of *MYB26* (B), *NST1* (C), *OPR3* (D), and *MYB24* (E) in wild-type and *arf17* flower buds at different floral developmental stages. The expression level in the wild-type and *arf17* flower buds was normalized to that of *TUB* and compared with the wild type at floral stages < 10. The anther and/or floral developmental stages refer to those of Sanders et al. (1999). The error bars indicate SDs and were calculated from three biological replicates. A two-tailed *t* test was used to evaluate statistical significance (*$P <$ 0.05; **$P <$ 0.01). F, Model of the auxin-ARF17-MYB108, JA, and ARF8-MYB26 pathway in regulating anther dehiscence.

role in anther dehiscence (Mandaokar and Browse, 2009), and we found that endothecium lignification was delayed in *myb108*, which is in agreement with its sterility at the early reproductive stage (Fig. 3). Our results have clearly shown the direct regulation of *MYB108* expression in flowers by ARF17 (Fig. 2). The expression of *MYB108* in *arf17* partly rescued its endothecium lignification (Figs. 4 and 5). Thus, *MYB108* plays an important role for ARF17 to regulate endothecium lignification, but it is not the only player. Another important gene, *NST1*, was down-regulated in *arf17* (Fig. 6C). *NST1* has been reported to be involved in endothecium lignification and anther dehiscence (Yang et al., 2017). Therefore, ARF17 regulates *MYB108* and potentially other transcription factors for endothecium lignification.

Auxin is important for gametophytic and sporophytic development in anthers. Auxin perception mediated by *TRANSPORT INHIBITOR RESPONSE1*, *AFB1*, *AFB2*, and *AFB3* is required for the timely regulation of anther dehiscence and pollen maturation (Cecchetti et al., 2008, 2013). Auxin biosynthesis through *YUC2* and *YUC6* is also important for anther dehiscence (Cheng et al., 2006). As shown in Figure 3 in Yao et al. (2018), the *yuc2 yuc6* mutant exhibits defective anther dehiscence. In this paper, we further demonstrated the importance of auxin signaling transduction mediated by ARF17 in endothecium lignification, which was completely blocked in *arf17* (Figs. 1 and 3). Therefore, auxin regulates endothecium lignification for anther dehiscence through ARF17 during anther development. Application of exogenous auxin or

overexpression of *OsYUCCA4* prevents anther dehiscence (Wilson et al., 2011; Song et al., 2018). Excess auxin may repress the function of ARF17 or other ARFs, which may lead to anther indehiscence. This appeared similar to the growth regulation by auxin in apical hook development in Arabidopsis, where the quantity of auxin is an important factor in controlling auxin response for promoting or inhibiting growth (Cao et al., 2019). This demonstrates that anther dehiscence is precisely regulated by auxin. The ARF8.4-MYB26-NST1/NST2 genetic pathway also regulates endothecium lignification. Overexpression of *ARF8.4* results in premature endothecium lignification and anther dehiscence (Yang et al., 2017; Ghelli et al., 2018). Since *NST1* was also down-regulated in *arf17* (Fig. 6C), this pathway is also regulated by auxin. ARF6 and ARF8 promote anther dehiscence in floral buds (Nagpal et al., 2005), and *ARF17* is substantially up-regulated in single mutants of *arf6* and *arf8* anthers (Supplemental Fig. S6). However, expression of *ARF17* and *MYB108* is not significantly affected in the *arf6 arf8* double mutant (Supplemental Fig. S7). These points demonstrate auxin regulates endothecium lignification, and ARF17 is a key regulator. However, the detailed auxin signaling regulating this process needs to be further elucidated in future work.

In addition to auxin, JA, an important hormone in plant development and stress response, is also involved in the regulation of anther dehiscence. OPR3 is an enzyme in the JA pathway. The *opr3* mutant shows defects in stomium opening (Cecchetti et al., 2013). In *yuc2 yuc6* flowers and *arf17* anthers, *OPR3* expression is up-regulated (Fig. 6, A and D). This is consistent with previous reports of auxin negatively regulating JA biosynthesis in flowers (Cecchetti et al., 2013). This negative regulation may coordinate the processes of endothecium lignification and stomium opening for anther dehiscence.

Anthers consist of four independent locules. Each locule forms four different sporophytic cell layers from the inside to the outside: the innermost tapetum, the middle layer, the endothecium, and the outermost epidermis cell layers. Microspore mother cells (MMCs) undergo meiosis to form the microspore and further develop into mature pollen grains in the center of the locule. These sporophytic cell layers have important biological functions during pollen maturation (Scott et al., 2004; Wilson et al., 2011). Auxin is essential for anther development and pollen formation. Auxin produced by MMCs regulates early microspore development (Yao et al., 2018). ARF17 is the key factor involved in the auxin signaling pathway, as *DR5::GFP* is barely detected in *arf17* anthers (Yang et al., 2013). In MMCs, *ARF17* directly regulates the expression of *CALS5* for tetrad wall formation (Yang et al., 2013). During anther development, the tapetum supplies microspores with various materials and nutrients, including sporopollenin and Mg (Xu et al., 2015; Xiong et al., 2016). ARF17 expression is precisely regulated in the tapetum for its development and function (Wang et al., 2017). In this study, we demonstrated that ARF17 is expressed in the endothecium to regulate its lignification for anther dehiscence (Fig. 6F). During anther development, MMC, tapetal, and endothecium cells have different biological functions. The expression of ARF17 in these cells likely coordinates their development to ensure pollen development and pollen release.

## MATERIALS AND METHODS

### Plant Materials and Growth Conditions

Arabidopsis (*Arabidopsis thaliana*) wild-type plants, transgenic plants, and mutants were in the Col-0 ecotype background. The *arf17*, *yuc2 yuc6*, *arf6*, *arf8*, and *arf6 arf8* mutants were obtained from the laboratory of Z.-N.Y. The *myb108* mutant (SALK_024059) was purchased from the transfer DNA mutant pool of The Arabidopsis Information Resource database (www.arabidopsis.org). The seeds were sown on vermiculite and allowed to imbibe for 2 to 3 d. The plants were then grown under the conditions of 16 h light/8 h darkness in a growth chamber at approximately 22°C.

### Microscopy

The plants were imaged by a Cyber-shot T-20 digital camera (Sony; www.sony.com). For semithin sectioning and GUS staining section, the flower buds were fixed and embedded in paraffin or Spurr's resin. Sections were prepared by cutting the buds into a thickness of 6 mm (GUS staining section) or 1 $\mu$m (semithin seciton), after which they were incubated in a 0.01% (w/v) toluidine blue solution for 5 to 10 min at 42°C and then washed with water. The sections were then observed with an BX51 microscope (Olympus; www.olympus-global.com) under the bright field. For cellulose observations, anthers at stage 12 were cut for semithin sections and stained with Tinopal for 15 min (10 mg/mL; Sigma-Aldrich; www.sigmaaldrich.com) as described previously by Lou et al. (2014). Lignin autofluorescence and GFP signals in the anthers of *ARF17-GFP/arf17* plants were observed using an FV3000 confocal laser scanning microscope (Olympus).

### Electron Microscopy

For TEM examination, the flower buds were fixed in a fixative solution containing 0.1 M phosphate buffer (pH 7.2) and 2.5% (v/v) glutaraldehyde and then washed three times with phosphate-buffered saline (pH 7.4). The fixed single flower bud was subsequently stained with osmium solution. Afterward, the buds were dehydrated with ethyl alcohol, subjected to a treatment of propylene epoxide, embedded in Spurr's resin (Electron Microscopy Sciences; www.emsdiasum.com) and polymerized for 48 h at 60°C as described previously by Xu et al. (2015). Ultrathin sections were observed via TEM microscopy (JEOL; www.jeol.co.jp). For scanning electron microscopy observations, fresh pollen grains and anthers were coated with 8 nm of gold and observed under a JSM-840 microscope (JEOL).

### Plasmid Construction and Identification of Transgenic Plants

The *promoterARF17::MYB108* fragment was constructed by combining the *ARF17* promoter (ProARF17-F/R) and the *MYB108* coding sequence region (MYB108CDS-F/R) to complement the *arf17* mutant. The *arf17* mutant background of *promoterARF17::MYB108* (*pARF17::MYB108*) was identified by PCR using the ARF17LP/ARF17RP and ARF17LP/T-LB primer pairs. The *promoterMYB108::GUS* fragment was constructed with a 3974 bp (upstream of the start codon) fragment of the MYB108 promoter, which was cloned using the primer pair 108GUS-F/108GUS-R. The background of the *myb108* mutant was identified by PCR using primer pairs 108LP/108RP and 108LP/LB. *Thermococcus kodakaraensis* (KOD) DNA polymerase (Toyobo; www.toyobo.co.jp) was used for amplification, and a pCAMBIA1300 binary vector (Cambia; www.cambia.org) was used for cloning. The cloned fragments were verified by sequencing. The constructs were subsequently transformed into *Agrobacterium tumefaciens* GV3101 and screened using 50 mg/mL kanamycin, 40 mg/mL

gentamicin, and 50 mg/mL rifampicin at 28°C. The floral-dip method was used for transformation (Yang et al., 2013). The transgenic plants were selected using 20 mg/L hygromycin. All primer sequences used are provided in Supplemental Table S3.

## RT-qPCR

Total RNA was extracted from the flower buds and anthers from wild-type plants, transgenic plants, and mutants via a TRIzol kit (Thermo Fisher Scientific; www.thermoscientific.com). In accordance with the manufacturer's instructions (Toyobo; www.toyoboglobal.com), first-strand complementary DNA was synthesized. RT-qPCR was then performed on a Prism 7300 detection system (Applied Biosystems; www.appliedbiosystems.com) with SYBR Green I master mix (Toyobo). The expression of *ARF17*, *MYB108*, *OPR3*, *DAD1*, *ARF8*, *MYB24*, *MYB26*, and *NST1* was detected via the primer pairs listed in Supplemental Table S3. The RT-qPCR results are shown as the relative expression levels normalized to the expression of *TUBULIN BETA8* (*TUB*), which was used as a positive control (TUB-F/R), and three biological replicates were included for every experiment.

## EMSAs

EMSAs were performed in accordance with previously reported methods (Yang et al., 2013). To obtain purified ARF17 proteins for the EMSA experiments, the full-length *ARF17* gene was amplified using the primer pairs ARF17GST-F and ARF17GST-R and cloned into a pGEX-4T vector (GE Healthcare; www.gehealthcare.com) to produce a GST-ARF17 construct. Expression and purification of the fusion protein were performed according to the manufacturer's instructions. A 60-bp DNA fragment containing the AuxRE element (TGTCTC) in the *MYB108* regulatory region and a mutant *MYB108* probe were generated by PCR amplification. The fragment was labeled with biotin to serve as the detection probe. A fragment without biotin was used as the competitor probe. The EMSA was performed with a light shift chemiluminescent EMSA kit (Thermo Fisher Scientific). The binding reactions containing binding buffer were carried out as described previously by Yang et al. (2013). The subsequent processes were performed according to the manufacturer's instructions. A Tanon-5500 chemiluminescent imaging system (Tanon; www.biotanon.com) was used to capture the images.

## ChIP

The ChIP procedure was performed as described by Yang et al. (2013). The relevant primers used are listed in Supplemental Table S3.

## Microarrays

Microarray analysis was performed according to the methods of Lou et al. (2014). The young buds of wild-type plants and *arf17* mutants were immediately frozen in liquid nitrogen. A Low RNA Input Linear Amplification Kit (Agilent Technologies; www.agilent.com) was used to amplify and label the total RNA. 5-(3-Aminoallyl)-UTP (Thermo Fisher Scientific), cyanine 3 (Cy3) *N*-hydroxysuccinimide (NHS) ester, and Cy5 NHS ester were used based on the manufacturers' instructions. The labeled complementary RNA (cRNA) was purified via an RNeasy Mini Kit (Qiagen; www.qiagen.com). According to the manufacturer's instructions, each 44-K Arabidopsis oligo microarray slide was hybridized with 825 ng of Cy3-labeled cRNA and 825 ng of Cy5-labeled cRNA by using a Gene Expression hybridization kit (Agilent) in a hybridization oven (Agilent). The slides were scanned by an Agilent microarray scanner (Agilent) in conjunction with Feature Extraction software 10.7 (Agilent) using the default settings. Three biological replicates of independently grown materials were used. The raw data were normalized with a locally weighted scatter plot smoothing (Lowess) algorithm via Gene Spring Software 11.0 (Agilent).

## Accession Numbers

The sequence data from this article can be found in The Arabidopsis Information Resource or GenBank/EMBL database under the following accession numbers: ARF17, AT1G77850; MYB108, AT3G06490; ADPG1, AT3G57510; ADPG2, AT2G41850; QRT2, AT3G07970; ARF6, AT1G30330; ARF8, AT5G37020; DAD1, AT2G44810; OPR3, AT2G06050; MYB26, AT3G13890; MYB24, AT5G40350; NST1, AT2G46770.

## Supplemental Data

The following supplemental materials are available.

**Supplemental Figure S1.** The semithin sections of anthers of wild-type plants and *arf17* mutants.

**Supplemental Figure S2.** The expression levels of *ADPG1, ADPG2,* and *QRT2* in *arf17* mutants.

**Supplemental Figure S3.** The identification and phenotype of *myb108* mutants.

**Supplemental Figure S4.** The identification of positive *promoterARF17::-MYB108* transgenic plants in the *arf17* background.

**Supplemental Figure S5.** The expression levels of *ARF6* and *ARF8* in the anthers of *arf17* mutants.

**Supplemental Figure S6.** The expression levels of *ARF17* in the anthers of *arf6* and *arf8* mutants.

**Supplemental Figure S7.** The expression levels of *ARF17* and *MYB108* in *arf6 arf8* mutants.

**Supplemental Table S1.** List of down-regulated genes in *arf17* mutants.

**Supplemental Table S2.** List of the 110 genes containing AuxRE motifs within their promoters.

**Supplemental Table S3.** List of primers used in this study.

Received May 15, 2019; accepted July 13, 2019; published July 25, 2019.

## LITERATURE CITED

**Auxenfans T, Terryn C, Paës G** (2017) Seeing biomass recalcitrance through fluorescence. Sci Rep **7:** 8838

**Cao M, Chen R, Li P, Yu Y, Zheng R, Ge D, Zheng W, Wang X, Gu Y, Gelová Z, et al** (2019) TMK1-mediated auxin signalling regulates differential growth of the apical hook. Nature **568:** 240–243

**Cardarelli M, Costantino P** (2018) An auxin switch for male fertility. Nat Plants **4:** 408–409

**Cecchetti V, Altamura MM, Serino G, Pomponi M, Falasca G, Costantino P, Cardarelli M** (2007). ROX1, a gene induced by rolB, is involved in procambial cell proliferation and xylem differentiation in tobacco stamen. Plant J **49:** 27–37

**Cecchetti V, Altamura MM, Falasca G, Costantino P, Cardarelli M** (2008) Auxin regulates Arabidopsis anther dehiscence, pollen maturation, and filament elongation. Plant Cell **20:** 1760–1774

**Cecchetti V, Altamura MM, Brunetti P, Petrocelli V, Falasca G, Ljung K, Costantino P, Cardarelli M** (2013). Auxin controls *Arabidopsis* anther dehiscence by regulating endothecium lignification and jasmonic acid biosynthesis. Plant J **74:** 411–422

**Cecchetti V, Celebrin D, Napoli N, Ghelli R, Brunetti P, Costantino P, Cardarelli M** (2017) An auxin maximum in the middle layer controls stamen development and pollen maturation in *Arabidopsis*. New Phytol **213:** 1194–1207

**Cheng Y, Dai X, Zhao Y** (2006) Auxin biosynthesis by the YUCCA flavin monooxygenases controls the formation of floral organs and vascular tissues in *Arabidopsis*. Genes Dev **20:** 1790–1799

**Ellis CM, Nagpal P, Young JC, Hagen G, Guilfoyle TJ, Reed JW** (2005) AUXIN RESPONSE FACTOR1 and AUXIN RESPONSE FACTOR2 regulate senescence and floral organ abscission in *Arabidopsis thaliana*. Development **132:** 4563–4574

**Ghelli R, Brunetti P, Napoli N, De Paolis A, Cecchetti V, Tsuge T, Serino G, Matsui M, Mele G, Rinaldi G, et al** (2018) A newly identified flower-specific splice variant of *AUXIN RESPONSE FACTOR8* regulates stamen elongation and endothecium lignification in Arabidopsis. Plant Cell **30:** 620–637

**Goldberg RB, Beals TP, Sanders PM** (1993) Anther development: Basic principles and practical applications. Plant Cell **5:** 1217–1229

**Guilfoyle TJ, Hagen G** (2007) Auxin response factors. Curr Opin Plant Biol **10:** 453–460

**Higo K, Ugawa Y, Iwamoto M, Korenaga T** (1999) Plant cis-acting regulatory DNA elements (PLACE) database: 1999. Nucleic Acids Res **27:** 297–300

**Huang H, Gao H, Liu B, Qi T, Tong J, Xiao L, Xie D, Song S** (2017) *Arabidopsis MYB24* regulates jasmonate-mediated stamen development. Front Plant Sci **8:** 1525

**Ishiguro S, Kawai-Oda A, Ueda J, Nishida I, Okada K** (2001) The DEFECTIVE IN ANTHER DEHISCIENCE gene encodes a novel phospholipase A1 catalyzing the initial step of jasmonic acid biosynthesis, which synchronizes pollen maturation, anther dehiscence, and flower opening in Arabidopsis. Plant Cell **13:** 2191–2209

**Lou Y, Xu XF, Zhu J, Gu JN, Blackmore S, Yang ZN** (2014) The tapetal AHL family protein TEK determines nexine formation in the pollen wall. Nat Commun **5:** 3855

**Mandaokar A, Browse J** (2009) MYB108 acts together with MYB24 to regulate jasmonate-mediated stamen maturation in Arabidopsis. Plant Physiol **149:** 851–862

**Mitsuda N, Seki M, Shinozaki K, Ohme-Takagi M** (2005) The NAC transcription factors NST1 and NST2 of Arabidopsis regulate secondary wall thickenings and are required for anther dehiscence. Plant Cell **17:** 2993–3006

**Nagpal P, Ellis CM, Weber H, Ploense SE, Barkawi LS, Guilfoyle TJ, Hagen G, Alonso JM, Cohen JD, Farmer EE, et al** (2005) Auxin response factors ARF6 and ARF8 promote jasmonic acid production and flower maturation. Development **132:** 4107–4118

**Ogawa M, Kay P, Wilson S, Swain SM** (2009) ARABIDOPSIS DEHISCENCE ZONE POLYGALACTURONASE1 (ADPG1), ADPG2, and QUARTET2 are Polygalacturonases required for cell separation during reproductive development in Arabidopsis. Plant Cell **21:** 216–233

**Park JH, Halitschke R, Kim HB, Baldwin IT, Feldmann KA, Feyereisen R** (2002). A knock-out mutation in allene oxide synthase results in male sterility and defective wound signal transduction in *Arabidopsis* due to a block in jasmonic acid biosynthesis. Plant J **31:** 1–12.

**Remington DL, Vision TJ, Guilfoyle TJ, Reed JW** (2004) Contrasting modes of diversification in the Aux/IAA and ARF gene families. Plant Physiol **135:** 1738–1752

**Sanders PM, Bui AQ, Weterings K, McIntire KN, Hsu Y-C, Lee PY, Truong MT, Beals TP, Goldberg RB** (1999) Anther developmental defects in *Arabidopsis thaliana* male-sterile mutants. Sex Plant Reprod **11:** 297–322

**Sanders PM, Lee PY, Biesgen C, Boone JD, Beals TP, Weiler EW, Goldberg RB** (2000) The Arabidopsis DELAYED DEHISCENCE1 gene encodes an enzyme in the jasmonic acid synthesis pathway. Plant Cell **12:** 1041–1061

**Scott RJ, Spielman M, Dickinson HG** (2004) Stamen structure and function. Plant Cell **16**(Suppl): S46–S60

**Song S, Chen Y, Liu L, See YHB, Mao C, Gan Y, Yu H** (2018) OsFTIP7 determines auxin-mediated anther dehiscence in rice. Nat Plants **4:** 495–504

**Steiner-Lange S, Unte US, Eckstein L, Yang C, Wilson ZA, Schmelzer E, Dekker K, and Saedler H** (2003). Disruption of *Arabidopsis thaliana* MYB26 results in male sterility due to non-dehiscent anthers. Plant J **34:** 519–528.

**Stintzi A, Browse J** (2000) The *Arabidopsis* male-sterile mutant, opr3, lacks the 12-oxophytodienoic acid reductase required for jasmonate synthesis. Proc Natl Acad Sci USA **97:** 10625–10630

**Tabata R, Ikezaki M, Fujibe T, Aida M, Tian CE, Ueno Y, Yamamoto KT, Machida Y, Nakamura K, Ishiguro S** (2010) *Arabidopsis* auxin response factor6 and 8 regulate jasmonic acid biosynthesis and floral organ development via repression of class 1 KNOX genes. Plant Cell Physiol **51:** 164–175

**Twell D** (2011) Male gametogenesis and germline specification in flowering plants. Sex Plant Reprod **24:** 149–160

**von Malek B, van der Graaff E, Schneitz K, Keller B** (2002) The *Arabidopsis* male-sterile mutant dde2-2 is defective in the ALLENE OXIDE SYNTHASE gene encoding one of the key enzymes of the jasmonic acid biosynthesis pathway. Planta **216:** 187–192

**Wang B, Xue JS, Yu YH, Liu SQ, Zhang JX, Yao XZ, Liu ZX, Xu XF, Yang ZN** (2017) Fine regulation of ARF17 for anther development and pollen formation. BMC Plant Biol **17:** 243

**Wilson ZA, Song J, Taylor B, Yang C** (2011) The final split: The regulation of anther dehiscence. J Exp Bot **62:** 1633–1649

**Winter D, Vinegar B, Nahal H, Ammar R, Wilson GV, Provart NJ** (2007) An "Electronic Fluorescent Pictograph" browser for exploring and analyzing large-scale biological data sets. PLoS One **2:** e718

**Xiong SX, Lu JY, Lou Y, Teng XD, Gu JN, Zhang C, Shi QS, Yang ZN, Zhu J** (2016). The transcription factors MS188 and AMS form a complex to activate the expression of CYP703A2 for sporopollenin biosynthesis in *Arabidopsis thaliana*. Plant J **88:** 936–946

**Xu XF, Wang B, Lou Y, Han WJ, Lu JY, Li DD, Li LG, Zhu J, Yang ZN** (2015). Magnesium Transporter 5 plays an important role in Mg transport for male gametophyte development in Arabidopsis. Plant J **84:** 925–936

**Yang C, Song J, Ferguson AC, Klisch D, Simpson K, Mo R, Taylor B, Mitsuda N, Wilson ZA** (2017) Transcription factor MYB26 is key to spatial specificity in anther secondary thickening formation. Plant Physiol **175:** 333–350

**Yang J, Tian L, Sun MX, Huang XY, Zhu J, Guan YF, Jia QS, Yang ZN** (2013) AUXIN RESPONSE FACTOR17 is essential for pollen wall pattern formation in Arabidopsis. Plant Physiol **162:** 720–731

**Yao X, Tian L, Yang J, Zhao YN, Zhu YX, Dai X, Zhao Y, Yang ZN** (2018) Auxin production in diploid microsporocytes is necessary and sufficient for early stages of pollen development. PLoS Genet **14:** e1007397